AIAA JOURNAL
Vol. 39, No. 5, May 2001

Analytical/Experimental Behavior of Anisotropic Rectangular Panels Under Linearly Varying Combined Loads

Giulio Romeo* and Gianni Ferrero†
Politecnico di Torino, 10129 Turin, Italy

An analytical solution has been obtained for the buckling of anisotropic rectangular panels subjected to several combinations of uniform shear and linearly varying biaxial in-plane loads. The principle of stationary value of the total potential energy was used for determining the buckling load of symmetric laminates through the solution of an eigenvalue problem; clamped and simply supported boundary conditions along edges were introduced into the analysis. The analytical results are in good agreement with the results concerning isotropic plates and the few results on infinitely long anisotropic plates. The buckling load of panels under linearly varying biaxial in-plane loads is largely influenced by the transverse compression load and by the boundary conditions along the four edges. Because no experimental results were found in the open literature, several tests were carried out on a graphite–epoxy rectangular panel to verify buckling behavior under various loading conditions, 1) uniaxial compression, 2) biaxial compression, and 3) biaxial compression with uniform load in the longitudinal direction, and three transverse load conditions, 1) trapezoidal, 2) triangular, and 3) in-plane bending. The maximum transverse load was of the same value as the longitudinal compression load; the panel was clamped along the four edges. A numerical analysis was also carried out by using the MSC/NASTRAN/PATRAN finite element code. The analytical, numerical, and experimental results show extremely good correlation.

Nomenclature

A_{ij}, D_{ij}	=	extension and bending stiffness matrices
a, b	=	plate dimensions in x and y directions, respectively
E_{mn}	=	undetermined coefficients for w
E_1, E_2, G_{12}	=	Young's and in-plane shear moduli of the lamina
K_x, K_y	=	nondimensional parameters as defined by Eq. (6)
M, N	=	number of terms in the series for w
M_x, M_y	=	moments per unit length
m, n, p, q	=	half-wavelength integers
N_x, N_y, N_{xy}	=	forces per unit length
$N_{x\,\mathrm{cr}}$, $N_{y\,\mathrm{cr}}$	=	buckling load, per unit length, in x and y directions, respectively
w	=	out-of-plane deflection
X_m, Y_n	=	characteristic functions for w
α_m	=	$m\pi/a$
β	=	$(D_{12} + 2D_{66})/(D_{11}D_{22})^{1/2}$
β_n	=	$n\pi/b$
γ_y, γ_x	=	linear coefficients defining the distribution of in-plane loads
δ_i, ε_i	=	numerical constants defining the clamped–clamped beam functions
ν_{12}	=	Poisson's ratio of the lamina

Introduction

MANY analytical and experimental results are available in the literature on buckling and postbuckling behavior of composite panels. Most of the results published concern uniform in-plane loads applied along the edges.[1] In most cases, the experimental results reported concern uniaxial compression or shear load only; in very few reports results have been reported for a combination of biaxial compression and shear load applied simultaneously.[2] However, a linearly varying load applied along the panel edges (Fig. 1) has to be taken into consideration in the design of various aerospace structure elements: box–beam webs, for example, are subjected to combined in-plane bending, transverse compression (due to crushing loads), and uniform shear; fuselage panels or launch vehicle structures are also subjected to combined nonuniform loads. Some research has been carried out in the past on isotropic plates under these loading conditions.[3–6] The Rayleigh–Ritz method was used to determine the buckling load. Several interaction curves were obtained for various plate aspect ratios and load combinations, for both simply supported and clamped boundary conditions. The interaction curves reported indicate great reduction in the buckling bending stress when a transverse compression load is also applied. In regard to anisotropic panels subjected to linearly varying combined loads very little documentation is available. By the use of the Rayleigh–Ritz method, Rao[7] evaluated the buckling behavior of fiber-reinforced plastic rectangular sandwich panels, with all edges simply supported, under the combined action of biaxial compression, in-plane bending and shear. Nemeth[8,9] presented an exhaustive parametric study of the buckling behavior of infinitely long anisotropic plates. The Rayleigh–Ritz method was used for obtaining the numerous generic buckling-design charts, applicable to a broad class of infinitely long laminate panels. However, the trigonometric functions used for satisfying the clamped boundary conditions along the two long edges are not particularly suitable for shorter rectangular panels.

The principle of stationary value of the total potential energy has been used in the present paper for determining the buckling load of symmetric laminated panels that are simply supported, clamped along four edges, or in a combination of both conditions. The characteristic clamped–clamped beam functions have been used to satisfy boundary conditions better. A very good correlation with the few analytical results found in the literature has been obtained. Because no experimental results have been found on the loading conditions plotted in Fig. 1, applied to finite dimension laminates, the buckling load per unit width has been found for the described loading profiles; trapezoidal or triangular compression loads as well as in-plane bending loads applied on each side gave a good correlation between analytical, finite element method (FEM), and experimental solutions.

Theoretical Analysis

For many engineering applications, the in-plane dimensions-to-thickness ratio is greater than 35. In such cases, transverse shear

Received 15 October 1999; revision received 28 September 2000; accepted for publication 20 November 2000.

*Associate Professor of Aerospace Structure Analysis, Department of Aerospace Engineering, Corso Duca degli Abruzzi 24; romeo@athena.polito.it.

†Aerospace Engineer, Department of Aerospace Engineering.

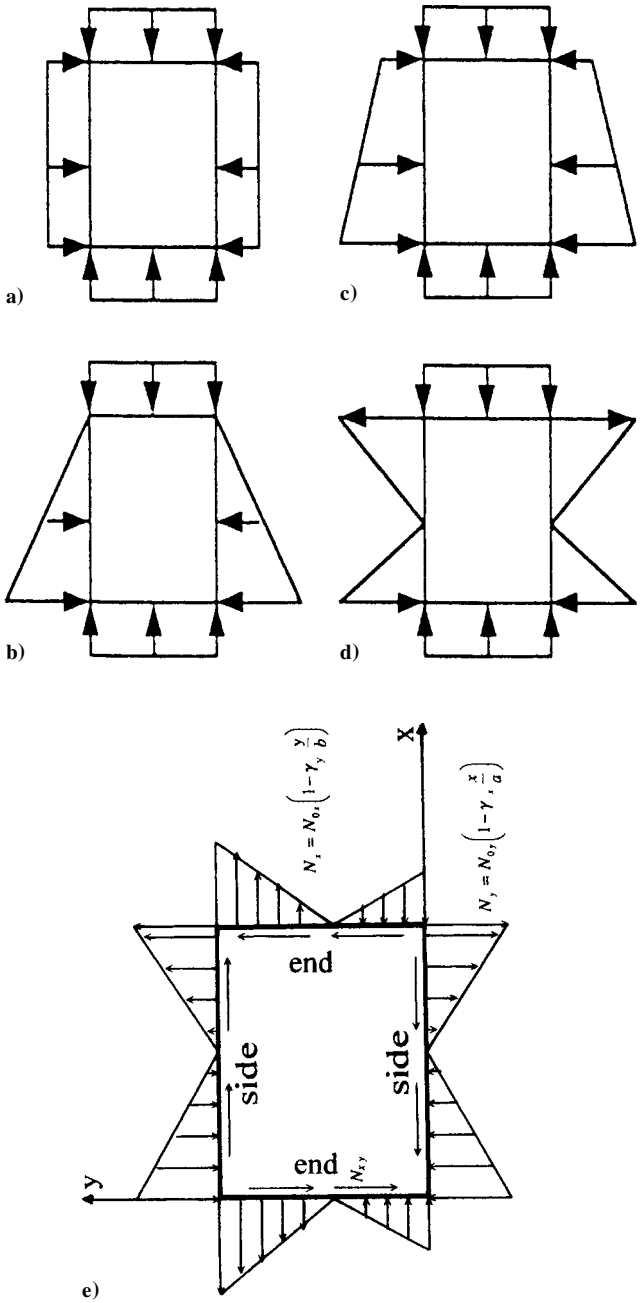

Fig. 1 Types of combined loading system applied to panel and geometry.

deformation will not affect laminate behavior significantly. Within the hypothesis of the classical lamination theory, by using the usual constitutive and kinematic relations,[1] it is possible to express the total potential energy of a balanced and symmetric laminate by the following equation (Fig. 1e):

$$V = \frac{1}{2}\int_0^a\int_0^b \Big[D_{11}w_{,xx}^2 + 2D_{12}w_{,xx}w_{,yy} + D_{22}w_{,yy}^2 + 4D_{66}w_{,xy}^2 + 4(D_{16}w_{,xx} + D_{26}w_{,yy})w_{,xy} + N_{x0}\left(1 - \frac{\gamma_y}{b}y\right)w_{,x}^2 + N_{y0}\left(1 - \frac{\gamma_x}{a}x\right)w_{,y}^2 - 2N_{xy}w_{,xy}\Big]\,dx\,dy \tag{1}$$

where γ_y and γ_x are linear coefficients defining the distribution of in-plane loads, $\gamma = 0$ is a uniform load (Fig. 1a), $\gamma = 0.5$ is a trapezoidal load (Fig. 1c), $\gamma = 1$ is a triangular load (Fig. 1b), and $\gamma = 2$ is an in-plane bending load (Fig. 1d). N_0 is the load for each edge, applied at the bottom of the panel. An index separated by a comma represents a derivative.

Four kinds of boundary conditions along the edges of the panel have been studied, satisfying the conditions reported here: 1) ends clamped-sides clamped (C–C):

$$x = 0, a: \quad w = w_{,x} = 0, \qquad y = 0, b: \quad w = w_{,y} = 0$$

2) ends simply supported–sides simply supported (S–S):

$$x = 0, a: \quad w = M_x = 0, \qquad y = 0, b: \quad w = M_y = 0$$

3) ends clamped–sides simply supported (S–C):

$$x = 0, a: \quad w = w_{,x} = 0, \qquad y = 0, b: \quad w = M_y = 0$$

and 4) ends simply supported–sides clamped (C–S):

$$x = 0, a: \quad w = M_x = 0, \qquad y = 0, b: \quad w = w_{,y} = 0$$

To satisfy the boundary conditions, the out-of-plane deflection has been expressed by a series:

$$w = \sum_m^M \sum_n^N E_{mn}X_m(x)Y_n(y) \tag{2}$$

where the characteristic X_m and Y_n functions assume the following expressions for simply supported or clamped condition, respectively.

Simply supported:

$$X_m(x) = \sin(m\pi x/a) = \sin\alpha_m x$$
$$Y_n(y) = \sin(n\pi y/b) = \sin\beta_n y \tag{3}$$

Clamped:

$$X_m(x) = \cosh(\varepsilon_m x/a) - \cos(\varepsilon_m x/a) - \delta_m[\sinh(\varepsilon_m x/a) - \sin(\varepsilon_m x/a)]$$
$$Y_n(y) = \cosh(\varepsilon_n y/b) - \cos(\varepsilon_n y/b) - \delta_n[\sinh(\varepsilon_n y/b) - \sin(\varepsilon_n y/b)] \tag{4}$$

The constants ε and δ have been determined with high precision (16 digits) to verify the following properties: $X_m(0) = X_m(a) = X_{m,x}(0) = X_{m,x}(a) = 0$ and $Y_n(0) = Y_n(b) = Y_{n,y}(0) = Y_{n,y}(b) = 0$.

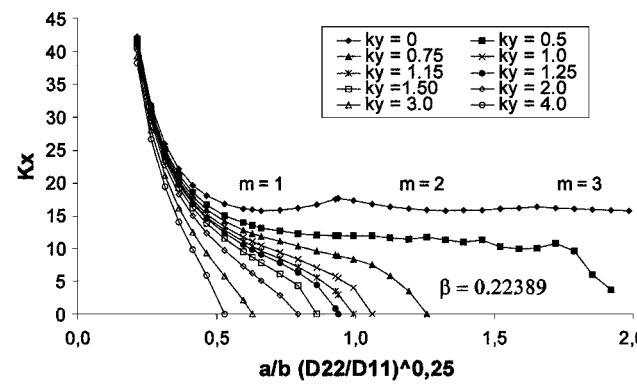

Fig. 2 Buckling results for simply supported orthotropic plates in combined longitudinal in-plane bending and transverse uniform compression loading.

Substituting expression (2), with proper boundary condition functions (3) or (4), into Eq. (1) and applying the principle of stationary value of the total potential energy with respect to the unknown coefficients E_{mn}, we obtain $(M \times N)$ linear equations similar to the following expression, valid for boundary condition number 4:

$$\frac{\partial V}{\partial E_{mn}} = \left[N_{x0}\frac{ab}{2}\alpha_m^2\left(1-\frac{\gamma_y}{2}\right) + N_{y0}\frac{a}{2b}\delta_n\varepsilon_n(\delta_n\varepsilon_n - 2) \times\left(1-\frac{\gamma_x}{2}\right)\right]E_{mn} + \sum_q^Q \left\{ -N_{x0}\gamma_y\frac{a}{b}\alpha_m^2\frac{8\delta_q\varepsilon_q^3/b^3\,\delta_n\varepsilon_n^3/b^3}{\left(\varepsilon_n^4/b^4 - \varepsilon_q^4/b^4\right)^2} \times[(-1)^{n+q}-1] + N_{y0}\left(1-\frac{\gamma_x}{2}\right)a\frac{2\varepsilon_q^2\varepsilon_n^2(\delta_q\varepsilon_q/b - \delta_n\varepsilon_n/b)}{\varepsilon_n^4 - \varepsilon_q^4} \times[(-1)^{n+q}+1]\right\}E_{mq} + \sum_p^P N_{y0}\gamma_x\frac{a}{b\pi^2}\frac{2mp}{(m^2-P^2)^2}\delta_n\varepsilon_n \times(\delta_n\varepsilon_n - 2)[1-(-1)^{m+p}]E_{pn} + \sum_p^P\sum_q^Q \left\{ -N_{xy}\frac{a}{\pi}\frac{4(\alpha_m p + \alpha_p m)}{m^2-p^2}\frac{\varepsilon_q^2\varepsilon_n^2}{\varepsilon_q^4-\varepsilon_n^4}[1-(-1)^{n+q}] + N_{y0}\gamma_x\frac{a}{\pi^2}\frac{8mp}{(m^2-p^2)^2}\frac{\varepsilon_q^2\varepsilon_n^2(\delta_q\varepsilon_q/b - \delta_n\varepsilon_n/b)}{\varepsilon_n^4-\varepsilon_q^4} \times[(-1)^{n+q}+1]\right\}[1-(-1)^{m+p}]E_{pq} + \left[D_{11}\frac{ab}{2}\alpha_m^4 + D_{22}\frac{a}{2b^3}\varepsilon_n^4 + (D_{12}+2D_{66})\frac{a}{b}\alpha_m^2\delta_n\varepsilon_n(\delta_n\varepsilon_n-2)\right]E_{mn} + \sum_q^Q(D_{12}+2D_{66}) \times a\alpha_m^2\frac{4\varepsilon_q^2\varepsilon_n^2(\delta_q\varepsilon_q/b - \delta_n\varepsilon_n/b)}{\left(\varepsilon_n^4-\varepsilon_q^4\right)}[(-1)^{n+q}+1]E_{mq} + \sum_p^P\sum_q^Q \left\{ -8\frac{D_{16}\alpha_m\alpha_p}{(m^2-p^2)}\frac{a}{\pi}\frac{\varepsilon_q^2\varepsilon_n^2}{\left(\varepsilon_n^4-\varepsilon_q^4\right)}[1-(-1)^{n+q}] \times(\alpha_m m + \alpha_p p) + 8\frac{D_{26}}{(m^2-p^2)}\frac{a}{b^2\pi}\frac{\varepsilon_q^3\varepsilon_n^3\delta_q\delta_n}{\left(\varepsilon_q^4-\varepsilon_n^4\right)}[1-(-1)^{n+q}] \times(\alpha_m p + \alpha_p m)\right\}[1-(-1)^{m+p}]E_{pq} = 0 \tag{5}$$

The computer program EMASTER5 was employed for working out the set of linear algebraic equations (5) in the form of a classical eigenvalue problem. By the extraction of the associated eigenvector, the buckling mode was also obtained. The EMASTER5 software operates on a Pentium II personal computer and requires very few seconds of CPU with 10×10 terms, using FORTRAN software.

Analytical Results

The theoretical results obtained by the present theory were first compared with the results concerning isotropic and anisotropic panels found in the literature[3–9] obtaining a very good agreement. The analytical results obtained for specially orthotropic panels (orthotropy parameter $\beta = 0.224$) under an in-plane bending load in the longitudinal direction, $\gamma = 2$, and a uniform compression load in the transverse direction (Fig. 1d) are shown in Fig. 2 as function of the plate aspect and orthotropic ratio. The following nondimensional parameters were introduced:

$$K_x = \frac{\left(N_{x\,\mathrm{cr}}b^2\right)}{\left[\pi^2(D_{11}D_{22})^{\frac{1}{2}}\right]}, \qquad k_y = \frac{\left(N_{y\,\mathrm{cr}}b^2\right)}{\left[\pi^2(D_{11}D_{22})^{\frac{1}{2}}\right]} \tag{6}$$

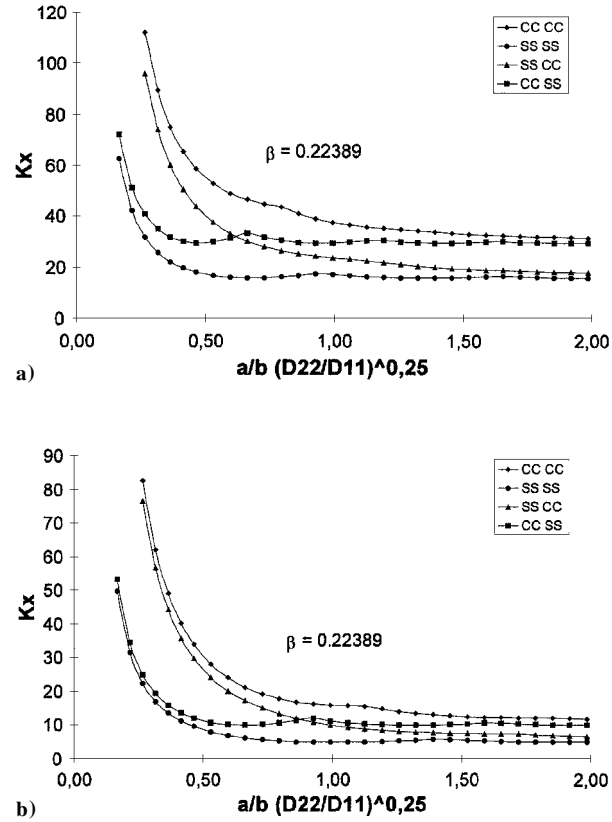

Fig. 3 Buckling results as function of boundary conditions and plate aspect ratio for orthotropic plates under a) longitudinal in-plane bending or b) triangular loading.

It is very clear that transverse compression has a great influence on the longitudinal bending buckling load. Increasing the compression has the marked effect of decreasing the in-plane bending buckling load, as well as of decreasing the number of half-waves in the direction of the bending stress.

The effects of boundary conditions and plate aspect ratio for specially orthotropic panels subjected to in-plane bending load or triangular load are shown in Fig. 3. As the plate aspect orthotropic ratio increases up to value one, the buckling load decreases drastically and the plate buckles into one or two half-waves in the longitudinal direction, depending on the boundary conditions. Subsequently the plate buckles into more buckle half-waves, and the buckling load slightly decreases.

All four boundary conditions were evaluated, and the following was noted: Panels with sides clamped and ends simply supported (CCSS), though starting with buckling coefficients similar to panels with all edges simply supported (at aspect ratio lower than 0.5), move toward the buckling coefficients of panels clamped along the four edges (CCCC) as panels become longer. The opposite behavior occurs in panels with sides simply supported and ends clamped (SSCC).

The effects of anisotropy for infinitely long angle ply panels subjected to in-plane bending and uniform shear are shown in Fig. 4, taken from Ref. 9. The following materials properties were used for the computations: $E_1 = 127.8$ GPa, $E_2 = 11.0$ GPa, $G_{12} = 5.7$ GPa, and $\nu_{12} = 0.35$. It is very clear that by neglecting the anisotropic terms D_{16} and D_{26} in the expression of total potential energy, a remarkable difference in the buckling coefficients can be obtained.

Experimental Results

Because no experimental results were found in the open literature, the test facility built at the Turin Polytechnical University[2–11] (Fig. 5) was implemented to apply the loading conditions plotted in Fig. 1 to panels with dimensions smaller than 1000×700 mm. The longitudinal load is applied to the panel by two separately controlled servoactuators (A in Fig. 5); a maximum load 250 kN in compression and 225 kN in tension can be applied by each actuator.

The transverse load application system, made up of two separately controlled servoactuators (B in Fig. 5), floats so as to not interfere with the longitudinal and shear load. A maximum load of 100 kN, in compression as well as in tension, can be applied by each actuator. The shear load is applied to the bottom end of the panel by a servoactuator (C in Fig. 5). A maximum positive or negative load of 200 kN can be applied. A displacement control is used to keep the panel ends parallel to each other, their angular rotation controlled to zero with an accuracy of 0.001 deg.

Several tests were carried out on a graphite–bismaleimide rectangular panel subjected to different combined loads to verify its buckling behavior. A T800-5250 prepreg tape was used to manufacture the panel with the following lay-up: $(45_2/90_5/-45_2/0_2/90_2)_{2s}$. The panel was vacuum bagged and autoclave cured for 6 h at 177°C and a pressure of 0.6 MPa. The materials properties used for the computations were experimentally determined to be $E_1 = 168.7$ GPa, $E_2 = 8.5$ GPa, $G_{12} = 5.9$ GPa, and $\nu_{12} = 0.335$.

The usable dimensions of the panel (when inserted in the steel L-profile test fixture), measured 880 mm in length and 580 mm in width. The panel was clamped along the four edges. To measure in-plane strains (Fig. 6a), 32 strain gauges, either linear or rosette, were back-to-back (e.g., 1,2; 3,4; etc.) bonded to the panel. The out-of-plane displacements were recorded by using seven inductive transducers (Fig. 6b), as well as the shadow-moiré method.

Several sequential tests were carried out on the panel, 1) uniaxial compression test, 2) biaxial compression test with a ratio of

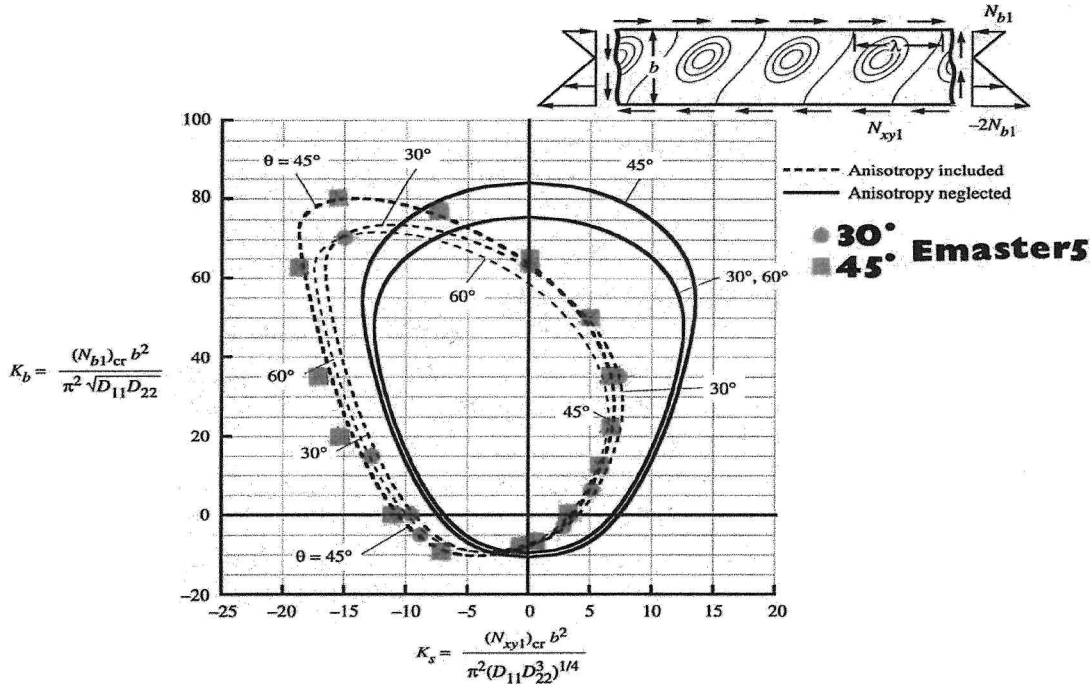

Fig. 4 Buckling results for infinitely long angle-ply laminate subjected to longitudinal in-plane bending and uniform shear loading; comparison with results of Fig. 20 of Ref. 9.

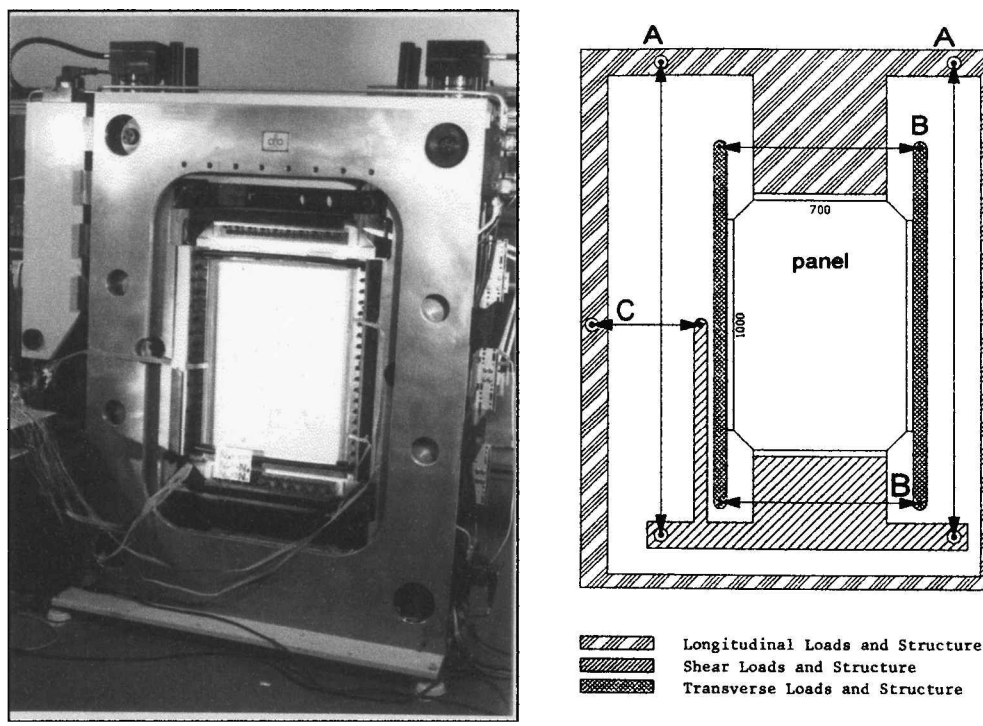

Fig. 5 Testing machine for application of linearly varying combined loading.

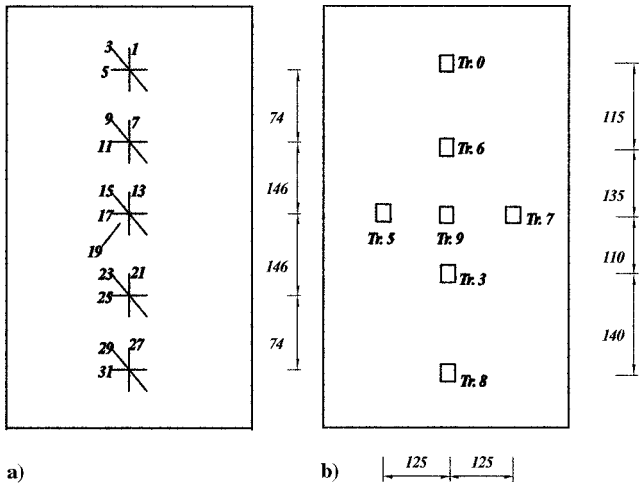

Fig. 6 a) Strain gauges location and b) Inductive transducers positioning. All dimensions are in millimeters.

transverse load per unit width to longitudinal load of 0.6, and 3) biaxial compression with uniform longitudinal load and three transverse load conditions: 1) trapezoidal, 2) triangular, and 3) in-plane bending. The maximum transverse load is of the same value as the compression load applied longitudinally. The higher transverse compression load is applied at the bottom of the panel.

The experimental results are shown in Figs. 7–9 for the panel under loading conditions 3–1, 3–2, and 3–3 described, respectively, in the preceding paragraph. For each loading condition, the applied longitudinal load is plotted as a function of strains in the longitudinal direction measured by back-to-back gauges placed in the upper part (gauges 1 and 2), central part (gauges 13 and 14), and lower part (gauges 27 and 28) of the panel. Strains measured in the transverse direction of the panel's lower part (gauges 31 and 32) are plotted in Figs. 7–9. Strains measured in the transverse direction of the panel's upper part (gauges 5 and 6) are plotted only in Fig. 9. The experimental critical load at which the panel displayed buckling was defined by the load vs strain curves as the value at which the transverse membrane strain (gauges 31 and 32) does not increase further. The qualitative representation of the out-of-plane

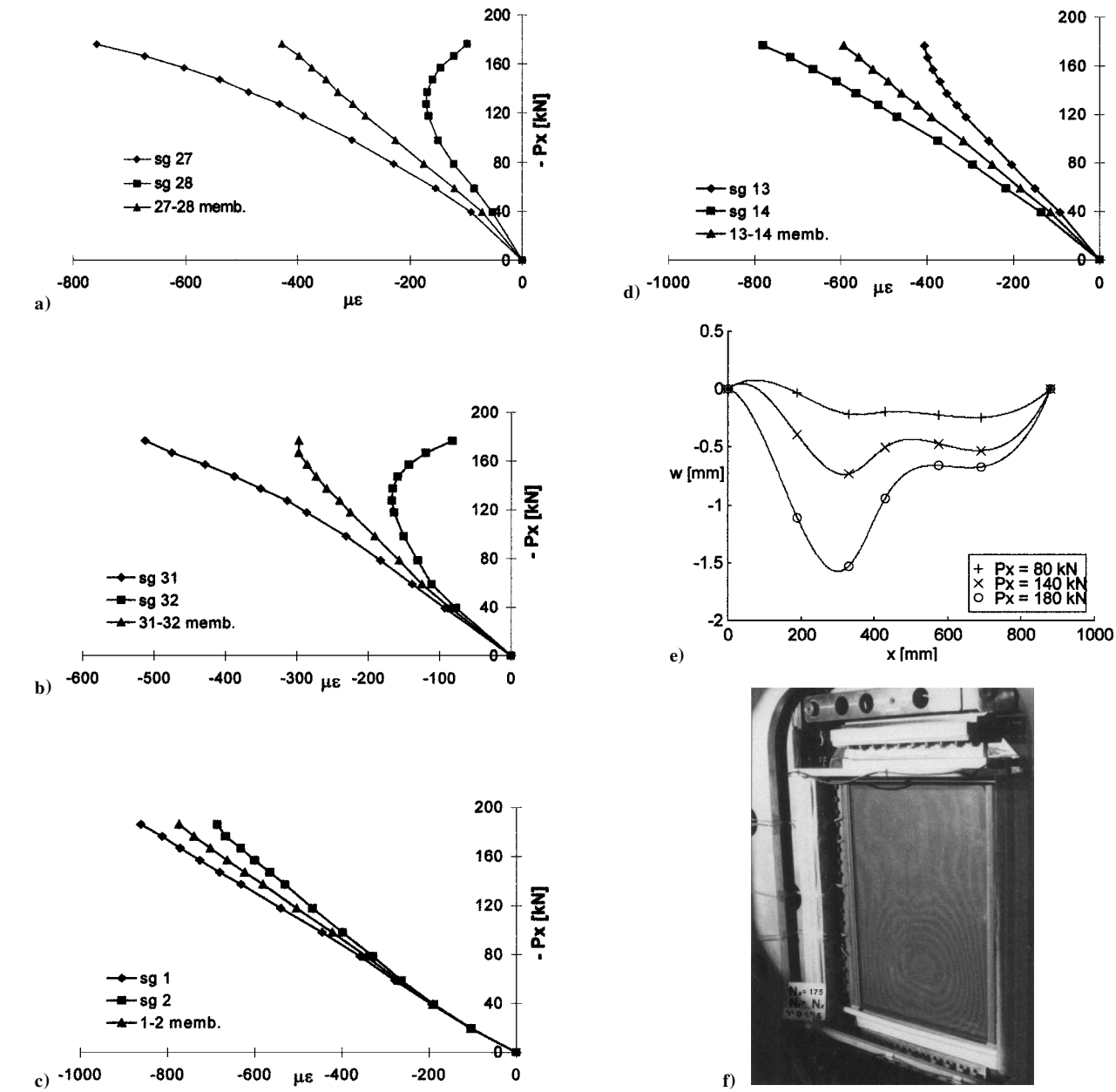

Fig. 7 Experimental results for a clamped anisotropic panel under uniform longitudinal compression and trapezoidal transverse compression loading; applied longitudinal load as a function of strain gauges: a) 27 and 28, b) 31 and 32, c) 1 and 2, d) 13 and 14; e) out-of-plane deflection along the longitudinal direction at several applied loads; and f) experimental shadow-moiré patterns at an applied longitudinal load of 175 kN.

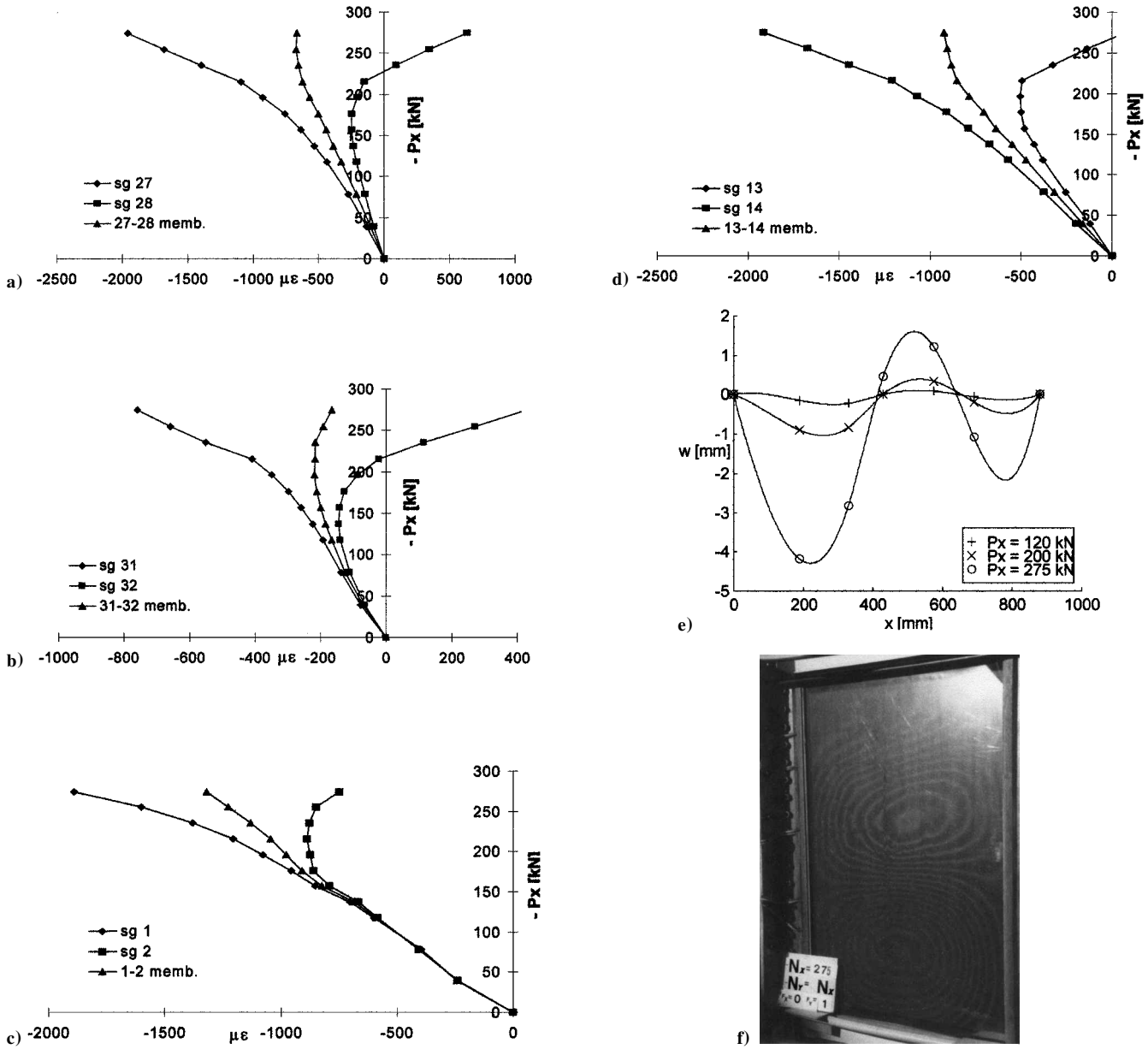

Fig. 8 Experimental results for a clamped anisotropic panel under uniform longitudinal compression and triangular transverse compression loading; applied longitudinal load as a function of strain gauges: a) 27 and 28, b) 31 and 32, c) 1 and 2, d) 13 and 14; e) out-of-plane deflection along the longitudinal direction at several applied loads; and f) experimental shadow-moiré patterns at an applied longitudinal load of 275 kN.

displacement obtained by the shadow-moiré method is reported as well as furthermore, the out-of-plane deflections measured by the transducers along the longitudinal middle section. The continuous curves plotted were obtained interpolating the experimental results by using a cubic spline.

When the panel was subjected to longitudinal uniform compression load and trapezoidal transverse compression load (Fig. 7), the bottom half of the panel displayed buckling behavior at 166.6 kN, as shown clearly by the constant value of membrane transverse strain recorded by gauges 31 and 32. The longitudinal membrane strains, recorded by gauges 27 and 28, continued to increase, although an evident surface strain reversal occurred at about the same load. The upper part of the panel, however, was still in the prebuckling field, as clearly shown by the longitudinal strains measured by gauges 1 and 2, while a surface strain reversal started at the maximum applied load. The panel buckled in two half-waves. Perhaps because of a slight initial imperfection, the upper wave was not well developed.

Experimental results obtained for the panel subjected to longitudinal uniform compression load and triangular transverse compression load are shown in Fig. 8; about the same behavior was recorded as for the preceding, test, but for different loads. Because a higher load was applied, the upper part of the panel evidenced a surface strain reversal; a measured strain greater than in the previous test was reached. The panel buckled in three half-waves, each of them with different out-of-plane deflections.

Experimental results obtained for the panel subjected to longitudinal uniform compression load and in-plane bending transverse load are shown in Fig. 9. A transverse tensile strain was measured in the upper part of the panel (gauges 5 and 6) because of the transverse tensile load applied. Nevertheless, a surface strain reversal (gauges 1 and 2) was starting in the longitudinal direction. The bottom half of the panel, as seen from the measurements of both transverse and longitudinal gauges (31 and 32 and 27 and 28), was clearly in the buckling field. The panel buckled in three half-waves, recording its largest out-of-plane deflections in the bottom part of the panel.

A summary of the buckling results is shown in Table 1, including the analytical buckling load obtained by means of the present theory and the numerical results obtained by the NASTRAN code (as discussed later). The buckling load of the panel decreased as we moved from uniaxial compression to uniform biaxial compression (a 17% reduction). A 26% reduction of the buckling load was recorded when the trapezoidal load was applied transversally. With respect to the uniform biaxial compression test, however, the maximum transverse load applied gave the same value as the longitudinal

Table 1 Analytical, experimental, and FEM longitudinal buckling load P_x (kN) of the panel under different combined loads ($\gamma_y = 0$)

Applied load			EMASTER5			NASTRAN		
N_{x0}/N_{x0}	N_{y0}/N_{x0}	γ_x	S–S	C–C	C–S	C–C	C–S	Experimental
−1	0	0	−108.9	−222.4	−194.6	−247.5	−212.9	−225.4
−1	−0.6	0	−71.9	−177.9	−163.8	−198.7	−179.3	−186.5
−1	−1	0.5	−62	−166.3	−150.0	−158.6	−142.6	−166.6
−1	−1	1	−72.5	−180.2	−157.3	−176.2	−153.4	−176.4
−1	−1	2	−88.5	−205.8	−170.3	−195.7	−158.7	−196.0

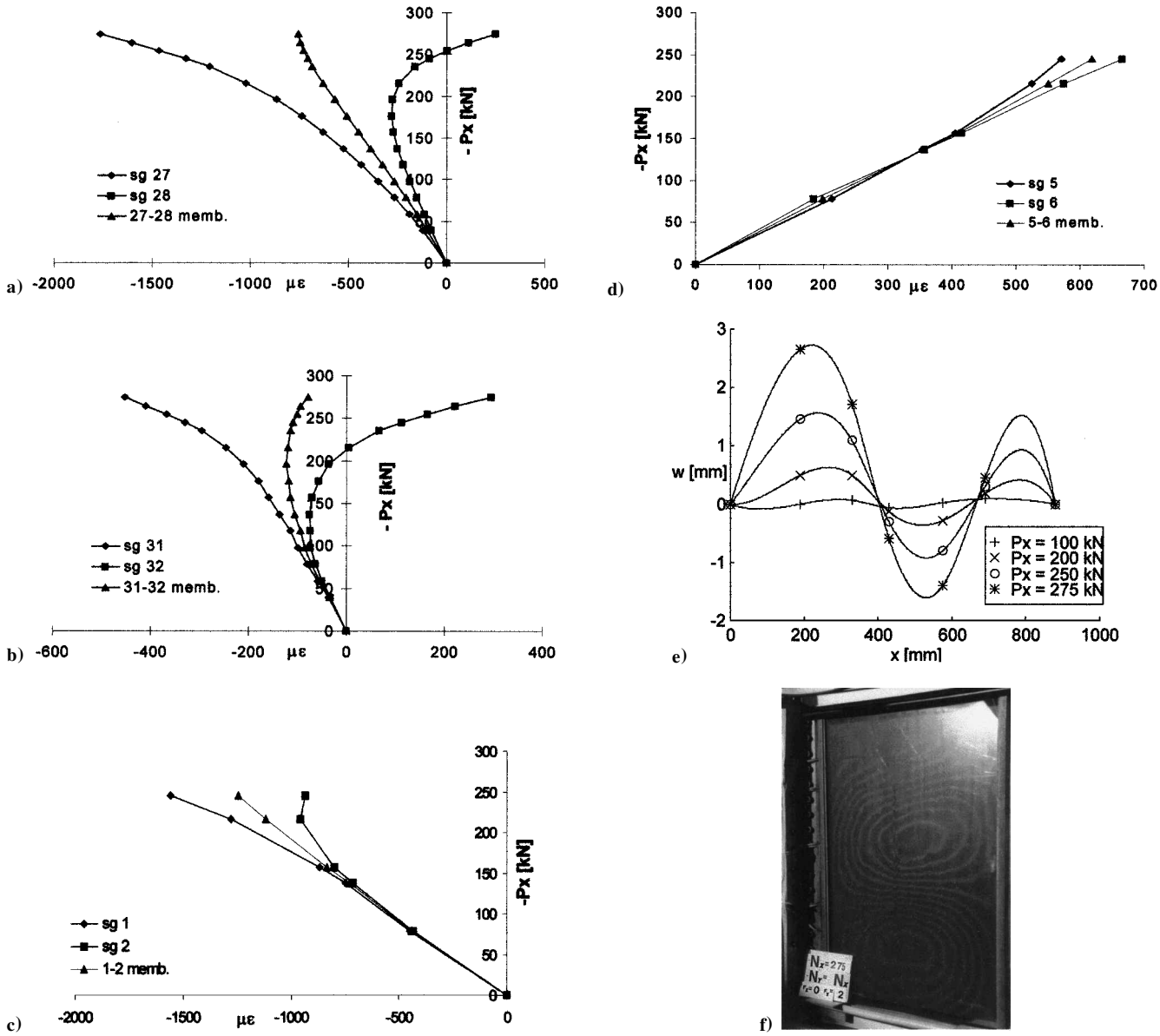

Fig. 9 Experimental results for a clamped anisotropic panel under uniform longitudinal compression and in-plane bending transverse loading; applied longitudinal load as a function of strain gauges: a) 27 and 28, b) 31 and 32, c) 1 and 2, d) 5 and 6; e) out-of-plane deflection along the longitudinal direction at several applied loads; and f) experimental shadow-moiré patterns at an applied longitudinal load of 275 kN.

load. Both the triangular and the in-plane bending load (applied transversally) again increased the buckling load with respect to the trapezoidal load. A 22% reduction and a 13% reduction, respectively, were recorded, as compared to the uniaxial compression test.

Comparison Between Analytical, Numerical, and Experimental Results

Various analytical and numerical results have been obtained from the panel tested under different load and boundary conditions. The theoretical analysis reported earlier and the EMASTER5 program were used for obtaining the analytical results. The load at which buckling is bound to occur is reported in Table 1. Three kinds of boundary conditions along the edges of the panel were considered: ends and sides simply supported, ends and sides clamped, and ends simply supported and sides clamped.

The MSC/NASTRAN finite element code was used, in conjunction with the MSC-PATRAN code as prepost processor, for obtaining the numerical results. The panel was modeled with 5336 elements, each defined by 8 nodes, CQUAD8 type. The upper end

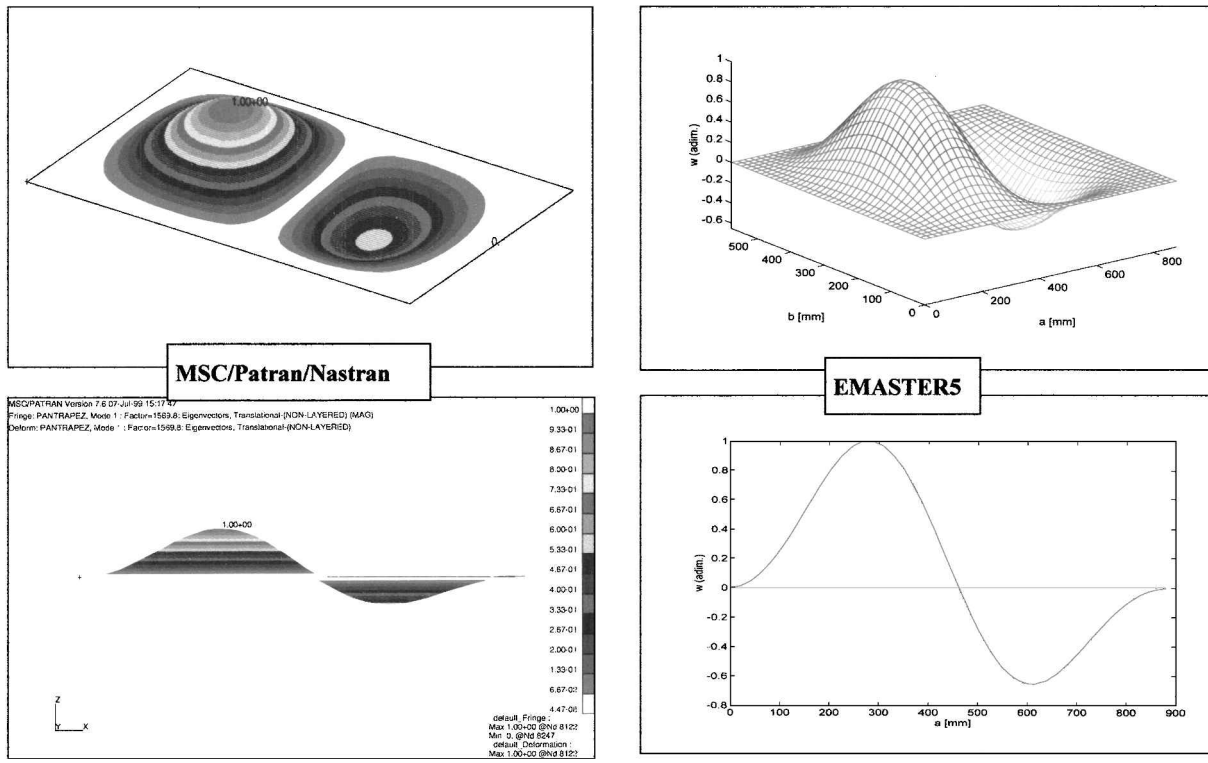

Fig. 10 Theoretical (EMASTER5) and numerical (NASTRAN) out-of-plane deflection for a clamped anisotropic panel under uniform longitudinal compression and trapezoidal transverse compression loading.

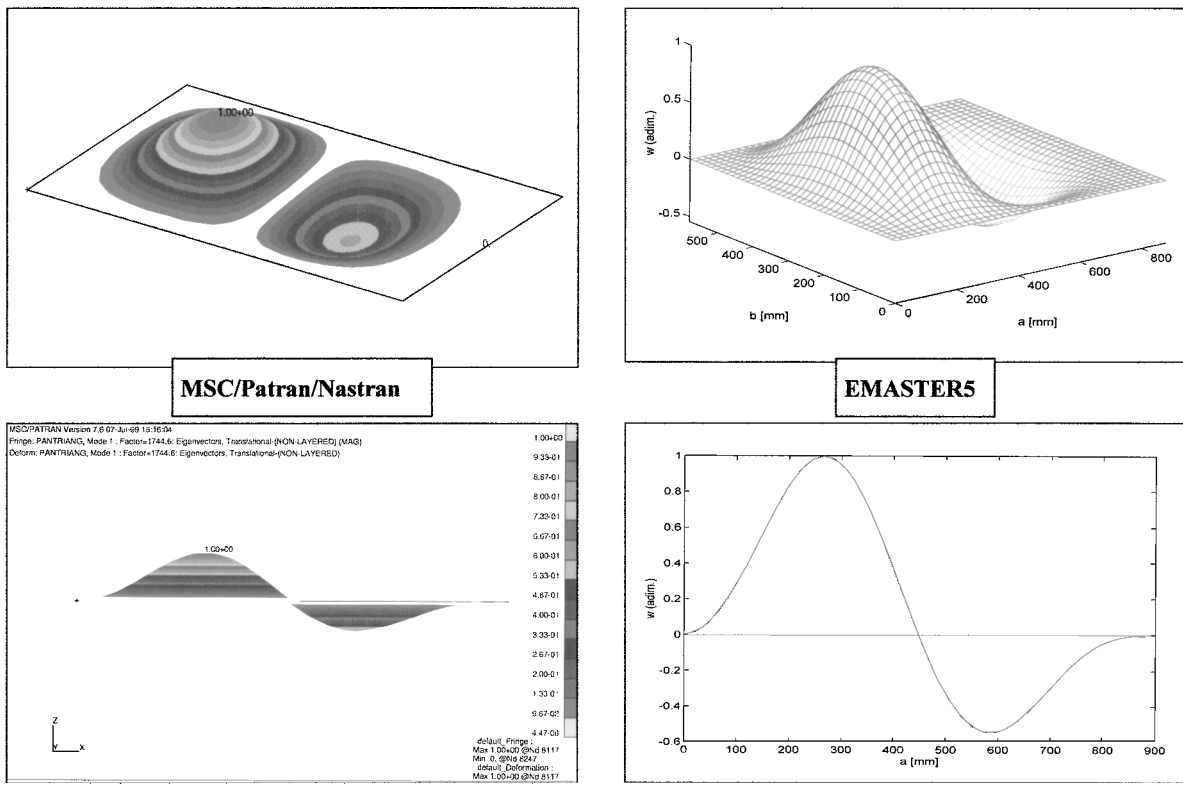

Fig. 11 Theoretical (EMASTER5) and numerical (NASTRAN) out-of-plane deflection for a clamped anisotropic panel under uniform longitudinal compression and triangular transverse compression loading.

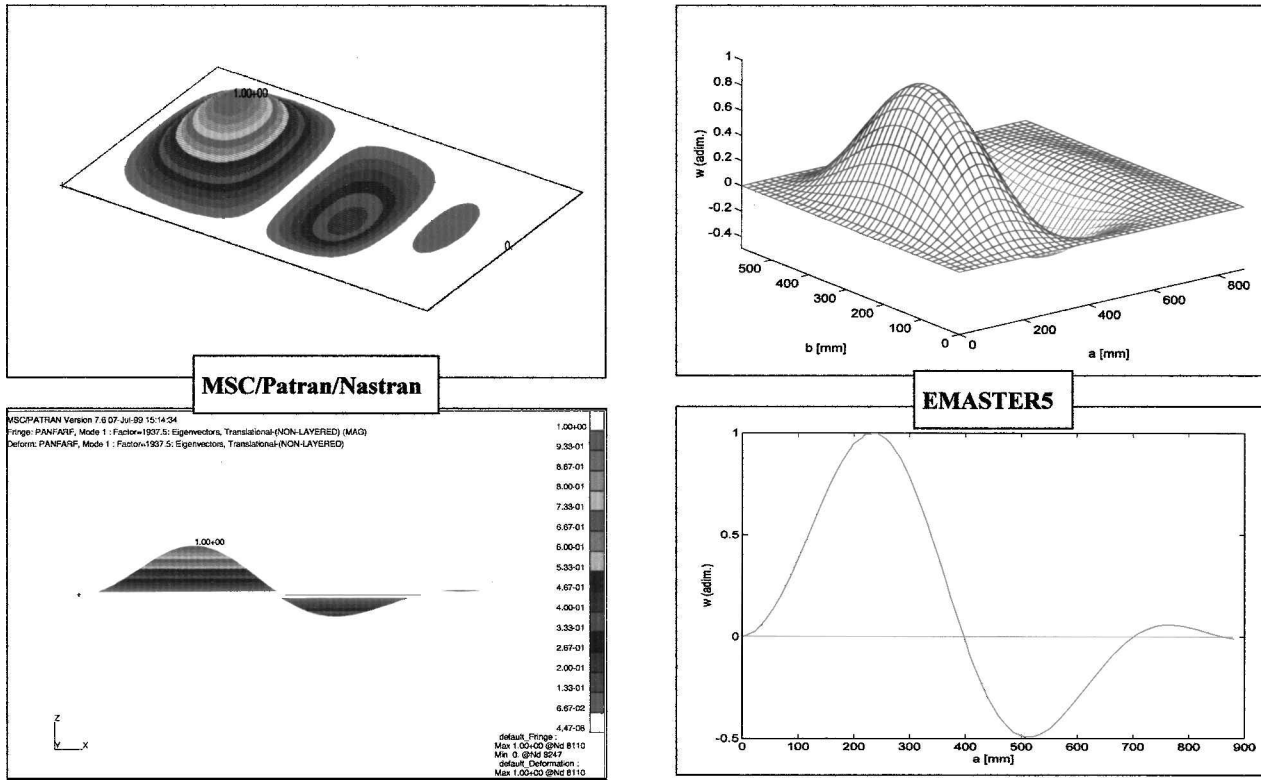

Fig. 12 Theoretical (EMASTER5) and numerical (NASTRAN) out-of-plane deflection for a clamped anisotropic panel under uniform longitudinal compression and in-plane bending transverse loading.

of the panel has no translation, whereas the lower end moves. Out-of-plane deflection was not allowed along the four edges, nor was rotation allowed along the four edges when all were clamped (only along two sides in the second case reported in Table 1). A very good correlation was obtained between analytical and numerical results when the panel was subjected to a linearly variable load. A difference of up to 10% was obtained when a uniform load was applied to the panel. From the comparison between the present analysis, the MSC/NASTRAN, and the experimental results (reported in Table 1), it is obvious that a very good agreement occurs when the panel is considered clamped along the four edges. A difference of up to 10% was recorded with respect to the numerical result only when the panel was subjected to uniaxial compression.

The out-of plane deflections of the panel under uniform longitudinal compression and linearly varying transverse loads are reported in Figs. 10–12. The axonometric views and deflections along the longitudinal middle section (as obtained by EMASTER5 as well as by the NASTRAN code) are shown in Figs. 10–12. The experimental out-of-plane deflections have already been shown in Figs. 7–9.

When subjected to longitudinal uniform compression load and trapezoidal transverse compression load (Fig. 10), the panel buckles in two half-waves; naturally a higher deflection is obtained in the bottom part of the panel because of the higher applied transverse compression load. Exactly the same behavior was obtained through the present theory and the NASTRAN code. The experimental deflection (Fig. 7), however, differs slightly from the theoretical results. Perhaps due to a slight initial imperfection, the upper wave was not well developed, but seemed to be increasing at the maximum applied load.

Also, when subjected to longitudinal uniform compression load and triangular transverse compression load (Fig. 11), the panel should buckle in two nonsymmetric half-waves, the computation by both codes giving exactly the same behavior. The experimental out-of-plane deflection (Fig. 8), however, differs from the theoretical results, recording a three half-wave buckling shape. Note that this buckling shape was also analytically obtained by both codes when the panel has ends simply supported and sides clamped.

When subjected to longitudinal uniform compression load and in-plane bending transverse load (Fig. 12), the panel should buckle in three half-waves, with a very little out-of-plane deflection in the upper part of the panel where the tensile load is applied transversally. Exactly the same behavior was obtained by both the EMASTER5 and the NASTRAN codes. The experimental deflection (Fig. 9) differs slightly from the theoretical results. Possibly because of the method used for interpolating the experimental data, the upper wave was observed to be larger than the value predicted analytically.

Conclusions

An analytical solution was obtained for panels clamped or simply supported along their edges when subjected to linearly variable edge loads. The buckling load was determined by the principle of stationary value of total potential. From the comparison with the few results found in the literature and with the numerical and experimental results obtained for the first time with the device specially developed at our university, it is possible to confirm the accuracy of the method. The many results obtained show how the buckling load of panels subjected to trapezoidal, triangular, and bending load is largely influenced by the transverse compression load and by the boundary conditions along the four edges. Further research may be directed to tests in which also a shear load is applied to the panel. Before this can be attempted, a new panel needs to be manufactured with the proper design of the corners.

Acknowledgments

The authors acknowledge the efficacious cooperation of G. Frulla and L. Fattore.

References

[1]Whitney, J. M., *Structural Analysis of Laminated Anisotropic Plates*, Technomic, Basel, 1987.

[2]Romeo, G., and Frulla, G., "Nonlinear Analysis of Anisotropic Plates with Initial Imperfections and Various Boundary Conditions Subjected to Combined Biaxial Compression and Shear Loads," *International Journal of Solids and Structures*, Vol. 31, No. 6, 1994, pp. 763–783.

[3]Grossman, N., "Elastic Stability of Simply Supported Flat Rectangular Plates Under Critical Combinations of Transverse Compression and Longitudinal Bending," *Journal of the Aeronautical Sciences*, Vol. 16, No. 5, 1949, pp. 272–276.

[4]Noel, R. G., "Elastic Stability of Simply Supported Flat Rectangular Plates Under Critical Combinations of Longitudinal Bending, Longitudinal Compression and Lateral Compression," *Journal of the Aeronautical Sciences*, Vol. 19, No. 12, 1952, pp. 829–834.

[5]Timoshenko, S. P., and Gere, J. M., "Buckling of a Simply Supported Rectangular Plate Under Combined Bending and Compression," *Theory of Elastic Stability*, 2nd ed., McGraw–Hill, New York, 1961, pp. 373–379.

[6]Gerard, G., and Becker, H., "Handbook of Structural Stability. Part I—Buckling of Flat Plates," NACA TN-3781, July 1957.

[7]Rao, K. M., "Buckling Coefficients for Fiber-Reinforced Plastic-Faced Sandwich Plates Under Combined Loading," *AIAA Journal*, Vol. 25, No. 5, 1987, pp. 733–739.

[8]Nemeth, M. P., "Buckling Behavior of Long Anisotropic Plates Subjected to Combined Loads," NASA TP-3568, Nov. 1995.

[9]Nemeth, M. P., "Buckling Behavior of Long Symmetrically Laminated Plates Subjected to Shear and Linearly Varying Axial Edge Loads," NASA TP-3659, July 1997.

[10]Romeo, G., and Frulla, G., "Experimental Behavior of Graphite/Epoxy Panels with Cut-Outs Under Biaxial Tension, Compression and Shear Loads," 21st Congress of the International Council of the Aeronautical Sciences, ICAS Paper 98-4,4,2, Sept. 1998.

[11]Romeo, G., and Frulla, G., "Postbuckling Behavior of Graphite/Epoxy Stiffened Panels with Initial Imperfections Subjected to Eccentric Biaxial Compression Loading," *International Journal of Non-Linear Mechanics*, Vol. 32, No. 6, 1977, pp. 1017–1033.

A. M. Waas
Associate Editor